

Syntheses and Magnetic Properties of Two New Tungstocobalt Heteropoly Acid-Lanthanide Complexes¹

M. L. Liu^a,*, W. Gu^b, and X. Liu^b, **

^aTianjin Modern Vocational Technology College, Tianjin, 300350 P.R. China

^bDepartment of Chemistry, Nankai University, Tianjin, 300071 P.R. China

e-mail: *meilingliu@mail.nankai.edu.cn; **liuxin64@nankai.edu.cn

Received April 16, 2014

Abstract—Two new ionic complexes built on polyoxometalate anions of $[\text{CoW}_{12}\text{O}_{40}]^{6-}$ and Ln^{3+} ($\text{Ln} = \text{Ce, Nd}$) cations, namely $[\text{Ce}(\text{CoW}_{12}\text{O}_{40})(\text{NMP})_2(\text{H}_2\text{O})_6][\text{Ce}(\text{NMP})(\text{H}_2\text{O})_8] \cdot 3\text{H}_2\text{O} \cdot \text{NMP}$ (**I**) and $[\text{Nd}(\text{CoW}_{12}\text{O}_{40})(\text{NMP})_2(\text{H}_2\text{O})_6][\text{Nd}(\text{NMP})(\text{H}_2\text{O})_8] \cdot 7\text{H}_2\text{O}$ (**II**) ($\text{NMP} = \text{N-methyl-2-pyrrolidone}$) have been synthesized. Single crystal X-ray crystallographic analyses (CIF files CCDC nos. 704837 (**I**) and 689561 (**II**)) revealed that the structures of two complexes were similar, which crystallize in the $P2_1/n$ monoclinic space group. Complexes **I** and **II** were both ionic clusters and the coordination numbers of Ln^{3+} ($\text{Ln} = \text{Ce, Nd}$) were nine. The unit cell parameters for **I**: $a = 17.551(4)$, $b = 17.783(4)$, $c = 26.729(5)$ Å, $\beta = 101.33(3)^\circ$, $V = 8180(3)$ Å³, $Z = 4$. The unit cell parameters for **II**: $a = 17.571(3)$, $b = 17.750(3)$, $c = 28.989(9)$ Å, $\beta = 115.42(2)^\circ$, $V = 8166(3)$ Å³, $Z = 4$. Complex **I** was characterized by TG analysis. Variable-temperature magnetic susceptibility measurements showed that there exists a weak antiferromagnetic interaction of complex **II**.

DOI: 10.1134/S1070328414110049

INTRODUCTION

In recent years, in the field of solid-state chemistry, the design, synthesis and characterization of organic-inorganic hybrid materials have been attracting extensive interest because of the architectural beauty of their structures and potential application in such as catalysis, photochemistry, medicine, and so on [1–4]. Meanwhile, polyoxometalates (POMs) as one of the most important members in the family of organic-inorganic hybrid materials have also attracted more and more researchers' attention. So far, many intermolecular complexes based on polyoxometalates have been synthesized and reported [5–11]. Among those classical building structures, the found of Keggin-structure is an epoch-making event in the history of POMs. However, to our knowledge, lanthanide coordination polymers based on $[\text{CoW}_{12}\text{O}_{40}]^{6-}$ had never been reported previously.

In polyoxometalate chemistry, one of the major challenges is the “rational” synthesis of new compounds. From the standpoint of molecular design, we attempted to use normal synthesis to realize such molecular assemblies. Here, we chose lanthanide(III) ions (Ln^{3+}), which have potential uses in bioinorganic chemistry and materials science [12–14]. Then we chose NMP molecules as electron donors since polyoxometalate anions are good electron acceptors, which will lead to electron transfer. Here, we report

the syntheses and X-ray single crystal structure analyses of tungstocobalt heteropoly acid-lanthanide complexes: $[\text{Ce}(\text{CoW}_{12}\text{O}_{40})(\text{NMP})_2(\text{H}_2\text{O})_6][\text{Ce}(\text{NMP})(\text{H}_2\text{O})_8] \cdot 3\text{H}_2\text{O} \cdot \text{NMP}$ (**I**) and $[\text{Nd}(\text{CoW}_{12}\text{O}_{40})(\text{NMP})_2(\text{H}_2\text{O})_6][\text{Nd}(\text{NMP})(\text{H}_2\text{O})_8] \cdot 7\text{H}_2\text{O}$ (**II**). Meanwhile, complex **I** was characterized by TG analysis and magnetic properties of complex **II** had been studied.

EXPERIMENTAL

Materials and methods. All reagents were obtained from commercial sources and used without further purification. $\text{K}_5\text{CoW}_{12}\text{O}_{40} \cdot 20\text{H}_2\text{O}$ was prepared according to the literature method [15]. $\text{CeCl}_3 \cdot 6\text{H}_2\text{O}$ was prepared through adding concentrated HCl to Ce_2O_3 (99.9%). $\text{NdCl}_3 \cdot 6\text{H}_2\text{O}$ was prepared through adding concentrated HCl to Nd_2O_3 (99.9%). Elemental analyses for C, H and N were performed on a Heraeus Chn-Rapid instrument. Thermogravimetric analysis was performed in flowing N_2 atmosphere with the temperature range of 25–800°C on a PerkinElmer TAC7/DC analyzer with a heating rate of 10°C/min. The magnetic susceptibility measurements were carried out on a polycrystalline sample with a Quantum Design MPMS-XL5 SQUID magnetometer in the temperature range 2–300 K. Diamagnetic corrections were estimated from Pascals constants.

Synthesis of I. $\text{K}_5\text{CoW}_{12}\text{O}_{40} \cdot 20\text{H}_2\text{O}$ (0.692 g, 0.2 mmol) and $\text{CeCl}_3 \cdot 6\text{H}_2\text{O}$ (0.0709 g, 0.2 mmol) were dissolved in 15 mL water and the solution was

¹ The article is published in the original.

heated at a 80°C water bath until being dry. Then 2 mL NMP was added to dried solid with stirring until the mixture being paste. After standing for a while, the paste was dissolved in enough amount of $\text{CH}_3\text{CN}-\text{H}_2\text{O}$ mixture (3 : 2 v/v). Finally, the solution was filtered and left to evaporate at room temperature. One or two days later, yellow block crystals of **I** were collected with a yield of 53%.

For $\text{C}_{20}\text{H}_{39}\text{N}_4\text{O}_{61}\text{CoCe}_2\text{W}_{12}$

anal. calcd., %: C, 7.28; H, 2.23; N, 1.71.
Found, %: C, 7.32; H, 2.31; N, 1.69.

IR spectrum (KBr; ν , cm^{-1}): 3420 w, 1646 s, 1508 w, 952 s, 877 s, 773 s, 442 s.

Synthesis of II. Using $\text{NdCl}_3 \cdot 6\text{H}_2\text{O}$ (0.0718 g, 0.2 mmol) instead of $\text{CeCl}_3 \cdot 6\text{H}_2\text{O}$, complex **II** was synthesized with the similar method of **I**. Pink block crystals of **II** were collected with a yield of 61%.

For $\text{C}_{15}\text{H}_{33}\text{N}_3\text{O}_{63}\text{CoNd}_2\text{W}_{12}$

anal. calcd., %: C, 7.23; H, 2.21; N, 1.74.
Found, %: C, 7.22; H, 2.24; N, 1.69.

IR (KBr; ν , cm^{-1}): 3395 w, 1646 s, 1508 w, 949 s, 879 s, 770 s, 444 s.

X-ray crystal determination. Crystal data collection for complex **I** and **II** are performed on a Bruker SMART APEX-CCD with MoK_α radiation ($\lambda = 0.71073 \text{ \AA}$). The data were corrected for Lorentz-polarization effects, and absorption corrections were applied. All nonhydrogen atoms were refined anisotropically and all of the hydrogen atoms were generated geometrically and allowed to ride on their parent carbon atoms. The structures **I** and **II** were solved by direct methods. The structures were refined by using SHELXL-97 [16]. The crystallographic details for **I** and **II** are provided in Table 1, and selected bond lengths for **I** and **II** are given in Table 2. Supplementary material has been deposited with the Cambridge Crystallographic Data Centre (nos. 704837 (**I**) and 689561 (**II**); deposit@ccdc.cam.ac.uk or <http://www.ccdc.cam.ac.uk>).

RESULTS AND DISCUSSION

The crystal structures of **I** and **II** are similar. Complexes **I** and **II** are both ionic clusters, including $[\text{Ln}(\text{CoW}_{12}\text{O}_{40})(\text{NMP})_2(\text{H}_2\text{O})_6]^{3-}$ ($\text{Ln} = \text{Ce, Nd}$) anionic clusters, cationic $[\text{Ln}(\text{NMP})(\text{H}_2\text{O})_8]^{3+}$ ($\text{Ln} = \text{Ce, Nd}$) complexes, free water and NMP molecules in the crystal lattice. The differences were that there were three free water molecules and one free NMP in **I**, but there were only seven free water molecules in **II**. Now take **I** for example to describe their structures.

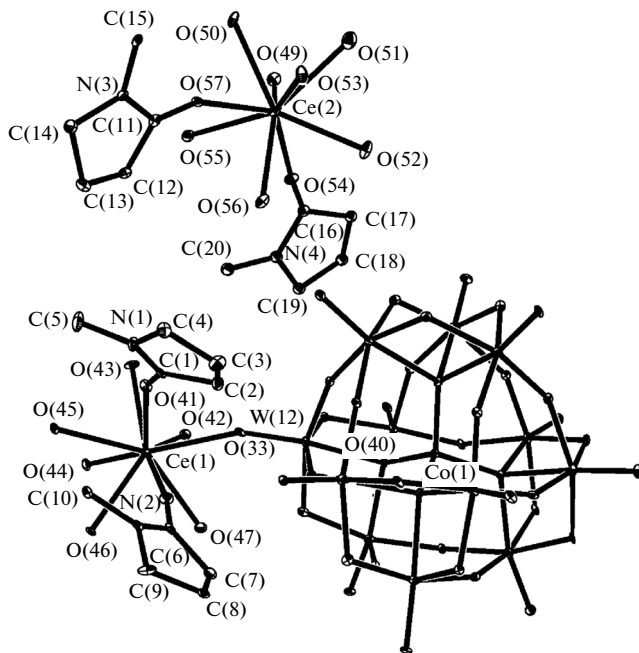


Fig. 1. The ORTEP representation of **I** with 10% (the hydrogen atoms are omitted for clarity).

The coordination environment of Ce^{3+} is shown in Fig. 1. The coordination numbers of the two Ce^{3+} ions are nine. Ce^{3+} in $[\text{Ce}(\text{CoW}_{12}\text{O}_{40})(\text{NMP})_2(\text{H}_2\text{O})_6]^{3-}$ anionic clusters is coordinated of one typical Keggin structural $[\text{CoW}_{12}\text{O}_{40}]^{6-}$ anion, two NMP and six water molecules. That means the nine coordinated O atoms were from one heteropolyanion, two NMP ligands, and the remaining seven O atoms are from seven water molecules, respectively. Ion Ce^{3+} in cationic $[\text{Ce}(\text{NMP})(\text{H}_2\text{O})_8]^{3+}$ complexes is coordinated of one NMP molecule and eight water molecules.

The coordination polyhedra around the Ce^{3+} ions can be described as a tricapped trigonal prism (Fig. 2), which is one of common coordination geometries for complexes with coordination number of nine [17]. In addition, the Ce–O bond distances range from 2.396 to 2.647 \AA , which is similar to the data of the reported references [18–23]. The Co–O bond distances range from 18.76 to 1.903 \AA for complex **I**, and the OCoO bond angels range from 109.1° to 110.03°. These results show that CoO_4 tetrahedrons are distorted to small extent.

Thermal stability of complex **I** was examined by TG analysis under N_2 atmosphere in the temperature range of 25–800°C (Fig. 3). TG curve shows that the host framework of the complex is thermally stable up to ~300°C. The first stage occurs at ~120°C with the weight loss of 6.0%, corresponding to the release of one free NMP molecule and three free water molecules (calcd. 6.8%). The second stage occurs at 490°C with the weight loss of 9.8%, which could be ascribed to the release of three coordinate NMP molecules

Table 1. Crystallographic data and structure refinement summary for **I** and **II**

Parameter	Value	
	I	II
Formula weight	3856.92	3816.93
Crystal system	Monoclinic	Monoclinic
Space group	<i>P</i> 2 ₁ / <i>n</i>	<i>P</i> 2 ₁ / <i>n</i>
<i>a</i> , Å	17.551(4)	17.571(3)
<i>b</i> , Å	17.783(4)	17.750(3)
<i>c</i> , Å	26.729(5)	28.989(9)
β, deg	101.33(3)	115.42(2)
<i>V</i> , Å ³	8180(3)	8166(3)
<i>Z</i>	4	4
ρ _{calcd} , g cm ⁻³	3.132	3.105
Absorption coefficient, mm ⁻¹	18.178	18.365
<i>F</i> (000)	6824	6729
Crystal size, nm	0.22 × 0.18 × 0.16	0.22 × 0.18 × 0.14
θ Range, deg	1.54–25.01	1.72–25.01
Limiting indices <i>h</i> , <i>k</i> , <i>l</i>	–20 ≤ <i>h</i> ≤ 20, –16 ≤ <i>k</i> ≤ 21, –34 ≤ <i>l</i> ≤ 31	–20 ≤ <i>h</i> ≤ 17, –21 ≤ <i>k</i> ≤ 19, –30 ≤ <i>l</i> ≤ 31
Scan mode	ω	ω
Reflections collected	46407	46668
Independent reflections (<i>R</i> _{int})	14405 (0.0875)	14340 (0.1559)
Reflections with (<i>I</i> > 2σ(<i>I</i>))	11605	10236
Parameters	911	868
GOOF	1.031	1.032
<i>T</i> , K	293(2)	293(2)
Final <i>R</i> indices (<i>I</i> > 2σ(<i>I</i>))	<i>R</i> ₁ = 0.0502, <i>wR</i> ₂ = 0.1244	<i>R</i> ₁ = 0.0943, <i>wR</i> ₂ = 0.2582
<i>R</i> indices (all data)	<i>R</i> ₁ = 0.0610, <i>wR</i> ₂ = 0.1294	<i>R</i> ₁ = 0.1241, <i>wR</i> ₂ = 0.2907
Largest diff. peak and hole, <i>e</i> Å ⁻³	4.415 and –2.169	5.619 and –7.347

Table 2. Selected bond lengths (Å) and angles (deg) for I and II

Bond	<i>d</i> , Å	Bond	<i>d</i> , Å
I			
Ce(1)–O(48)	2.396(7)	Ce(1)–O(46)	2.519(6)
Ce(1)–O(43)	2.455(7)	Ce(1)–O(33)	2.537(6)
Ce(1)–O(42)	2.547(7)	Ce(1)–O(41)	2.549(6)
Ce(1)–O(45)	2.571(7)	Ce(1)–O(47)	2.622(7)
Ce(1)–O(44)	2.575(6)	Ce(2)–O(54)	2.418(5)
Ce(2)–O(56)	2.509(8)	Ce(2)–O(50)	2.510(7)
Ce(2)–O(57)	2.511(7)	Co(1)–O(32)	1.876(6)
Ce(2)–O(55)	2.513(7)	Co(1)–O(40)	1.886(5)
Ce(2)–O(52)	2.517(7)	Co(1)–O(9)	1.891(6)
Ce(2)–O(51)	2.598(10)	Ce(2)–O(57)	2.511(7)
Ce(2)–O(49)	2.602(7)	Ce(2)–O(55)	2.513(7)
Ce(2)–O(53)	2.647(8)	Co(1)–O(32)	1.876(6)
Co(1)–O(16)	1.903(6)	Co(1)–O(40)	1.886(5)
II			
Nd(1)–O(48)	2.37(3)	Nd(2)–O(51)	2.61(3)
Nd(1)–O(43)	2.45(2)	Nd(2)–O(53)	2.63(2)
Nd(1)–O(33)	2.50(2)	Co(1)–O(32)	1.863(19)
Nd(1)–O(46)	2.52(3)	Co(1)–O(16)	1.874(16)
Nd(1)–O(45)	2.54(2)	Co(1)–O(9)	1.909(16)
Nd(1)–O(42)	2.57(2)	Co(1)–O(40)	1.936(19)
Nd(1)–O(44)	2.57(3)	Nd(2)–O(56)	2.46(2)
Nd(1)–O(41)	2.57(3)	Nd(2)–O(51)	2.61(3)
Nd(1)–O(47)	2.59(2)	Nd(2)–O(54)	2.44(2)
Angle	ω , deg	Angle	ω , deg
I			
O(42)Ce(1)O(44)	66.7(2)	O(42)Ce(1)O(47)	68.8(2)
O(41)Ce(1)O(44)	131.6(2)	O(41)Ce(1)O(47)	138.0(2)
O(45)Ce(1)O(44)	73.9(2)	O(45)Ce(1)O(47)	142.3(2)
O(48)Ce(1)O(47)	76.2(3)	O(44)Ce(1)O(47)	90.4(2)
O(43)Ce(1)O(47)	137.1(3)	O(54)Ce(2)O(56)	72.4(2)
O(46)Ce(1)O(47)	73.4(2)	O(54)Ce(2)O(50)	134.4(2)
O(33)Ce(1)O(47)	71.1(2)	O(56)Ce(2)O(50)	140.3(2)
O(42)Ce(1)O(44)	66.7(2)	O(54)Ce(2)O(57)	129.9(2)
O(41)Ce(1)O(44)	131.6(2)	O(56)Ce(2)O(57)	71.4(2)
O(45)Ce(1)O(44)	73.9(2)	O(50)Ce(2)O(57)	69.0(2)
O(48)Ce(1)O(47)	76.2(3)	O(54)Ce(2)O(55)	72.9(2)
O(43)Ce(1)O(47)	137.1(3)	O(56)Ce(2)O(55)	81.8(2)
O(46)Ce(1)O(47)	73.4(2)	O(50)Ce(2)O(55)	81.3(2)
O(33)Ce(1)O(47)	71.1(2)	O(57)Ce(2)O(55)	68.6(2)
O(48)Ce(1)O(43)	137.5(3)	O(56)Ce(2)O(52)	70.9(3)
O(48)Ce(1)O(46)	67.7(2)	O(50)Ce(2)O(52)	136.2(2)
O(43)Ce(1)O(46)	135.9(2)	O(57)Ce(2)O(52)	123.2(2)
O(48)Ce(1)O(33)	75.4(2)	O(55)Ce(2)O(52)	142.0(2)
O(43)Ce(1)O(33)	90.5(2)	O(54)Ce(2)O(51)	107.0(3)
O(46)Ce(1)O(33)	133.5(2)	O(56)Ce(2)O(51)	138.0(3)
O(48)Ce(1)O(42)	138.8(3)	O(50)Ce(2)O(51)	70.5(3)
O(43)Ce(1)O(42)	68.8(2)	O(57)Ce(2)O(51)	123.1(3)
O(46)Ce(1)O(42)	119.4(2)	O(55)Ce(2)O(51)	139.4(3)
O(33)Ce(1)O(42)	73.2(2)	O(52)Ce(2)O(51)	68.9(3)
O(48)Ce(1)O(41)	71.9(2)	O(54)Ce(2)O(49)	144.0(2)
O(43)Ce(1)O(41)	65.8(2)	O(56)Ce(2)O(49)	84.8(2)
O(46)Ce(1)O(41)	116.7(2)	O(50)Ce(2)O(49)	80.4(2)
O(33)Ce(1)O(41)	75.0(2)	O(57)Ce(2)O(49)	63.4(2)
O(42)Ce(1)O(41)	123.3(2)	O(55)Ce(2)O(49)	131.9(2)
O(48)Ce(1)O(45)	91.3(3)	O(52)Ce(2)O(49)	72.3(2)
O(43)Ce(1)O(45)	74.3(2)	O(51)Ce(2)O(49)	72.0(3)

Table 2. (Contd.)

Angle	ω , deg	Angle	ω , deg
O(46)Ce(1)O(45)	69.0(2)	O(54)Ce(2)O(53)	66.1(2)
O(33)Ce(1)O(45)	140.44(19)	O(56)Ce(2)O(53)	135.7(2)
O(42)Ce(1)O(45)	129.8(2)	O(50)Ce(2)O(53)	70.4(2)
O(41)Ce(1)O(45)	65.4(2)	O(57)Ce(2)O(53)	126.4(2)
O(48)Ce(1)O(44)	135.7(2)	O(55)Ce(2)O(53)	71.9(2)
O(43)Ce(1)O(44)	79.2(2)	O(52)Ce(2)O(53)	110.3(2)
O(46)Ce(1)O(44)	68.0(2)	O(51)Ce(2)O(53)	71.5(3)
O(46)Ce(1)O(44)	68.0(2)	O(49)Ce(2)O(53)	139.0(2)
O(32)Co(1)O(40)	109.0(2)	O(32)Co(1)O(9)	109.2(3)
O(40)Co(1)O(9)	110.3(2)	O(32)Co(1)O(16)	109.0(3)
O(40)Co(1)O(16)	109.6(2)	O(9)Co(1)O(16)	109.6(3)
II			
O(48)Nd(1)O(43)	135.7(9)	O(57)Nd(2)O(52)	123.9(6)
O(48)Nd(1)O(33)	71.2(8)	O(57)Nd(2)O(52)	123.9(6)
O(43)Nd(1)O(33)	92.6(8)	O(50)Nd(2)O(52)	136.2(9)
O(48)Nd(1)O(46)	71.2(9)	O(55)Nd(2)O(52)	140.6(7)
O(43)Nd(1)O(46)	135.4(8)	O(55)Nd(2)O(52)	140.6(7)
O(33)Nd(1)O(46)	132.0(7)	O(57)Nd(2)O(49)	62.8(7)
O(48)Nd(1)O(45)	92.3(8)	O(56)Nd(2)O(49)	85.8(7)
O(43)Nd(1)O(45)	73.8(7)	O(50)Nd(2)O(49)	79.4(8)
O(33)Nd(1)O(45)	140.0(7)	O(55)Nd(2)O(49)	132.3(7)
O(46)Nd(1)O(45)	69.8(7)	O(55)Nd(2)O(49)	132.3(7)
O(48)Nd(1)O(42)	136.2(8)	O(54)Nd(2)O(51)	104.7(8)
O(43)Nd(1)O(42)	69.6(7)	O(57)Nd(2)O(51)	124.0(8)
O(33)Nd(1)O(42)	72.9(7)	O(56)Nd(2)O(51)	137.6(8)
O(46)Nd(1)O(42)	119.2(8)	O(50)Nd(2)O(51)	71.8(9)
O(45)Nd(1)O(42)	131.4(7)	O(55)Nd(2)O(51)	140.2(7)
O(48)Nd(1)O(44)	138.2(9)	O(52)Nd(2)O(51)	67.8(8)
O(43)Nd(1)O(44)	79.3(8)	O(49)Nd(2)O(51)	72.8(8)
O(33)Nd(1)O(44)	140.9(7)	O(54)Nd(2)O(53)	66.8(7)
O(46)Nd(1)O(44)	67.0(8)	O(57)Nd(2)O(53)	127.5(6)
O(45)Nd(1)O(44)	74.5(7)	O(56)Nd(2)O(53)	136.7(7)
O(42)Nd(1)O(44)	68.4(8)	O(50)Nd(2)O(53)	70.7(7)
O(48)Nd(1)O(41)	70.1(8)	O(55)Nd(2)O(53)	74.4(7)
O(43)Nd(1)O(41)	65.8(8)	O(52)Nd(2)O(53)	108.3(7)
O(33)Nd(1)O(41)	74.5(8)	O(49)Nd(2)O(53)	136.8(8)
O(46)Nd(1)O(41)	118.1(8)	O(51)Nd(2)O(53)	68.7(8)
O(32)Co(1)O(16)	110.2(8)	O(32)Co(1)O(40)	109.6(8)
O(16)Co(1)O(40)	109.5(9)	O(32)Co(1)O(9)	108.3(8)
O(16)Co(1)O(9)	108.7(7)	O(40)Co(1)O(9)	110.5(8)
O(48)Nd(1)O(43)	135.7(9)	O(57)Nd(2)O(52)	123.9(6)
O(48)Nd(1)O(33)	71.2(8)	O(57)Nd(2)O(52)	123.9(6)
O(43)Nd(1)O(33)	92.6(8)	O(50)Nd(2)O(52)	136.2(9)
O(48)Nd(1)O(46)	71.2(9)	O(55)Nd(2)O(52)	140.6(7)
O(56)Nd(2)O(50)	140.2(7)	O(56)Nd(2)O(55)	80.7(7)
O(54)Nd(2)O(55)	72.7(7)	O(50)Nd(2)O(55)	82.6(8)
O(57)Nd(2)O(55)	69.5(6)	O(54)Nd(2)O(52)	72.9(7)

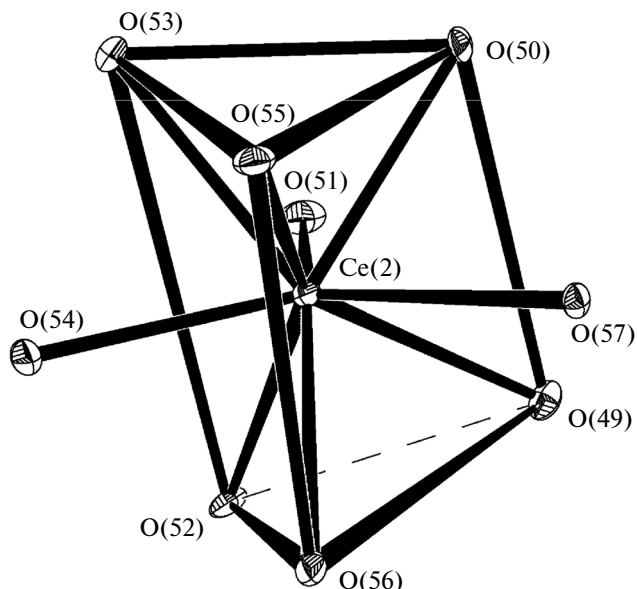


Fig. 2. Coordination polyhedron around Ce^{3+} in I.

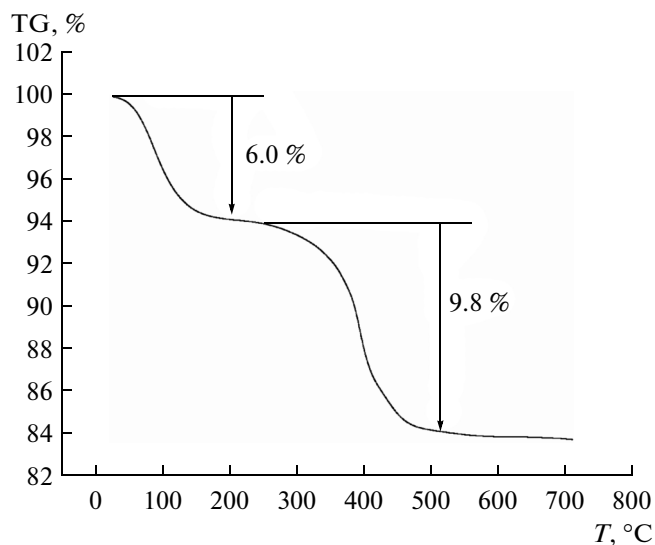


Fig. 3. TGA curves for I under a nitrogen flow.

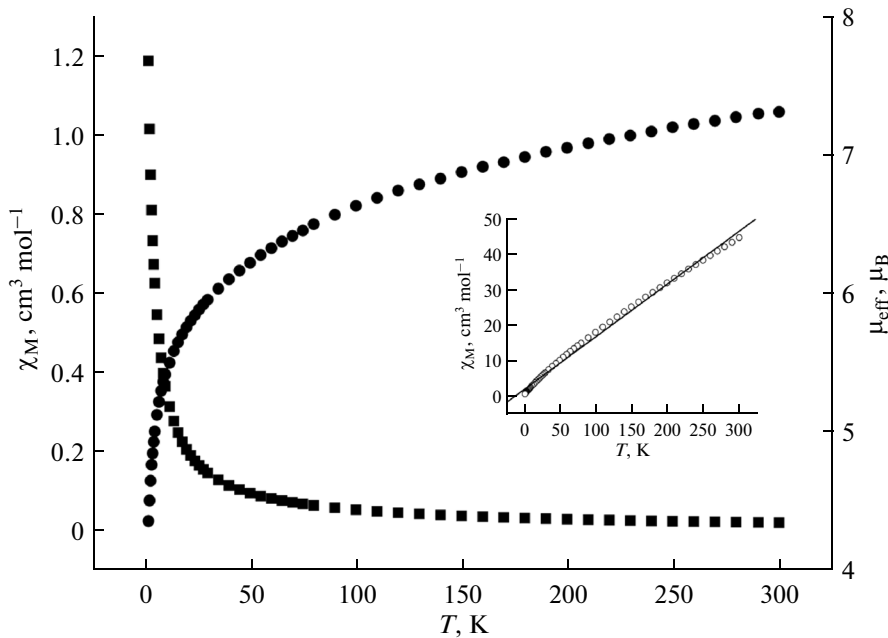


Fig. 4. Plots of the μ_{eff} (●) and χ_M (■) versus T for II.

(calcd. 9.6%). The sample keeps relatively stable in the range of 490–800°C and the remaining weight (84.2%) indicates that the final residue may be $\text{Ce}_2\text{CoW}_{12}\text{O}_{40}(\text{H}_2\text{O})_{14}$.

The spin orbital coupling in general plays an important role in the magnetism of lanthanide compounds due to the internal nature of the valence of orbits. This large spin orbit coupling partly removes the degeneracy of the ^{2S+1}L group term of lanthanide ions, giving $^{2S+1}\text{L}_J$ states, which further split into stark

levels under the crystal field perturbation [24]. The variable temperature magnetic susceptibilities were measured at an applied magnetic field of 1000 Oe in the temperature range of 2300 K for II. And the μ_{eff} vs. T plots are shown in Fig. 4. For complex II, the μ_{eff} value at 300 K of $7.45 \mu_{\text{B}}$ is similar with the plus of one isolated Nd^{3+} ion in the $^4I_{9/2}$ ($g = 8/11$) state and one isolated Co^{2+} , and it gradually decreases with decreasing temperature to reach a minimum of $4.32 \mu_{\text{B}}$ at 2 K. The decrease of the μ_{eff} product suggests the presence

of weak antiferromagnetic interaction. The low temperature decrease is likely due to a combination of the depopulation of Stark levels of Nd^{3+} ions and the presence of interlayer antiferromagnetic interactions. From 2 to 300 K, the data can be roughly fitted to a Curie-Weiss law with $C = 6.4 \text{ cm}^3 \text{ K mol}^{-1}$ and $\theta = -13.19 \text{ K}$. The Weiss constant is negative which also indicated that the dominant magnetic interaction is antiferromagnetic.

ACKNOWLEDGMENTS

This work was supported by the National Natural Science Foundation of China (nos. 21071083 and 20771062).

REFERENCES

1. Hill, C.L., *Chem. Rev.*, 1998, vol. 1, no. 2, p. 131.
2. Hill, C.L. and Prosser-McCartha, C.M., *Coord. Chem. Rev.*, 1995, vol. 143, p. 407.
3. Chesnut, D.J., Hagrman, D., Zapf, P.J., et al., *Coord. Chem. Rev.*, 1999, vol. 737, p. 190.
4. Nakagwa, Y., Uehara, K., and Mizuno, N., *Inorg. Chem.*, 2005, vol. 44, p. 14.
5. Niu, J.Y., Wu, Q., and Wang, J.P., *Dalton, Trans.*, 2002, vol. 12, p. 2512.
6. Niu, J.Y., You, X.Z., Duan, C.Y., et al., *Inorg. Chem.*, 1996, vol. 35, p. 4221.
7. GomezGarsia, C.J., Ouahab, L., Gimenez-Saiz, C., et al., *Angew. Chem., Int. Ed.*, 1994, vol. 33, p. 223.
8. GomezGarsia, C.J., Gimenez-Saiz, C., Triki, S., et al., *Inorg. Chem.*, 1995, vol. 34, p. 4139.
9. Galan-Mascaros, J.R., Gimenez-Saiz, C., Triki, S., et al., *Angew. Chem., Int. Ed.*, 1995, vol. 24, p. 1460.
10. Evans, H.T., *Biochemistry of Lanthanides*, New York: Plenum, 1990.
11. Yan, B.B., Xu, Y., Bu, X.H., et al., *Dalton Trans.*, 2001, vol. 7, p. 2009.
12. Evans, C.H., *Biochemistry of Lanthanides*, New York: Plenum, 1990.
13. Spedding, F.H., in *Kirk-Othmer Encyclopedia of Chemical Technology*, Grays, M. and Eckroth D., Eds., New York: Wiley, 1982, vol. 19, p. 883.
14. *Lanthanide Probes in Life, Chemical and Earth Sciences*, Bünzli, J.C.G. and Choppin, G.R., Eds., Amsterdam: Elsevier, 1989.
15. Guo, S.R. and Yao, N.L., *J. Chifeng. Univ.*, 2010, vol. 11, p. 26.
16. Sheldrick, G.M., *SHELX-97*, Göttingen (Germany): Univ. of Göttingen, 1997.
17. Lescop, C., Belorizky, E., Luneau, D., and Rey, P., *Inorg. Chem.*, 2002, vol. 41, p. 496.
18. Kannan, S., Gamare, J.S., Chetty, K.V., et al., *Polyhedron*, 2007, vol. 26, p. 3810.
19. Go, Y.B. and Jacobson, A.J., *Chem. Mater.*, 2007, vol. 19, p. 4702.
20. Gottfriesen, J., Spoida, M., and Blaurock, S., *Z. Anorg. Allg. Chem.*, 2008, vol. 634, p. 514.
21. Boyle, T.J., Tribby, L.J., and Bunge, S.D., *Eur. J. Inorg. Chem.*, 2006, vol. 11, p. 4553.
22. Seitz, M., Pluth, M.D., and Raymond, K.N., *Inorg. Chem.*, 2007, vol. 46, p. 351.
23. Katada, H., Seino, H., and Mizobe, Y., *Inorg. Chem.*, 2008, vol. 13, p. 249.
24. Wang, X.J., Cen, Z.M., Ni, Q.L., et al., *Cryst. Growth Des.*, 2010, vol. 10, p. 2960.